Bollettino di Geofisica Teorica ed Applicata Vol. 52, n. 2, pp. x-xx; June 2011
DOI 10.4430/bgta0007

Some aspects about surface wave and HVSR analyses: a short overview and a case study

G. Dal Moro

Eliosoft, Palmanova (UD), Italy
(previously GUtech - German University of Technology, Sultanate of Oman)

(Received: April 6, 2010; accepted: December 19, 2010)

ABSTRACT The present paper deals with some often poorly considered aspects related to data interpretation (and inversion) and non-uniqueness of solution when analysing seismic data according to methodologies based on surface wave propagation. Critical aspects are highlighted by presenting both synthetic and field data sets. A case study is presented with the aim of showing some complexities related to data analyses. The recommended holistic approach (joint analysis) is presented with a twofold goal. On one side improving the subsurface model, on the other helping in data interpretation/modelling for complex data sets. Since, ambiguities in velocity spectrum interpretation and non-uniqueness of the solution, do not make it possible to consider ReMi analyses as a solution for improving penetration depth, joint analyses of Rayleigh and Love-wave dispersion curves obtained from active seismics (also exploiting possible higher modes) and horizontal-to-vertical spectral ratio are considered together with compressional and shear wave refraction travel times capable of further validating V_S and V_P values for the shallowest layers. Rayleigh wave attenuation is also considered as an additional tool for retrieving the overall consistency of the subsurface model.

Key words: Surface waves, Rayleigh and Love wave dispersion, data inversion, HVSR, joint analyses, refraction, Rayleigh wave attenuation.

1. Introduction

In the last few decades, Surface Wave (SW) analysis has appeared as an appealing method for near-surface imaging (Stokoe *et al.*, 1988; Glangeaud *et al.*, 1999; Park *et al.*, 1999; Shtivelman, 1999, 2002; Xia *et al.*, 1999, 2004; Louie, 2001; O'Neill *et al.*, 2006; Dal Moro *et al.*, 2007). Classical refraction studies based on body wave analysis have thus found a significant aid able to partially overcome some well-known limitations mainly related to low-velocity channel(s) and blind layer(s).

Surface wave dispersion can be analysed by considering either an active or a passive experimental setting. The acronym MASW (Multichannel Analysis of Surface Waves), although it could in principle indicate any kind of geophone-array-based study, is normally used for the active case while ReMi (Refraction Microtremors) commonly refers to linear-array passive experiments.

HVSR (Horizontal-to-Vertical Spectral Ratio) is also sometimes proposed as a tool for depicting the vertical V_S profile, although the debate is still open about some problematic points

that characterize its phenomenology thus its possible use for unambiguous subsurface investigations (e.g., Fah *et al.*, 2001; Bonnefoy-Claudet *et al.*, 2008).

Of course, no method can be considered as the ultimate stand-alone solution both for intrinsic general limitations and site-specific problematic aspects that can limit specific methodologies. A critical point relates to the fact that analyses always require data interpretation and final results dramatically depend on it. On the other hand, it must be bear in mind that any automatic procedure that is now and then proposed is necessarily based on some assumptions that, althoughcan be valid under some circumstances however, cannot be considered universally applicable.

The present paper is aimed at briefly summarizing some problematic aspects of the mentioned methods thus showing that the only possible approach for a sound non-invasive investigation is the holistic one. Data interpretation (thus modelling/inversion) must in fact identify a model able to properly justify all the observed data.

After putting in evidence some often poorly considered aspects of surface wave analysis, a non-trivial case study is presented.

2. One method, no sound solution

Albeit researchers often long for a final solution able to image the subsurface materials under any circumstance, non-invasive surface investigations are inevitably subject to ambiguities in the retrieved model. In other words, the observed data sets can often be explained by different subsurface models.

This aspect is often neglected by many authors and consequently poorly understood by the end users.

It is important to underline that any (seismic and non-seismic) methodology suffers from this problem (Scales *et al.*, 2001). Ivanov *et al.* (2005a, 2005b) emphasized, for instance, the well-known problems of the blind layer and velocity inversion channel in refraction seismics. Luke *et al.* (2003) and Dal Moro *et al.* (2007), have already put in evidence the fact that dispersion curves also suffer from a relevant non-uniqueness problem.

The presence of several local minima in the inversion process is quite well-known. Fig. 1 synthesizes the consequent problem of the starting model that affects gradient-based inversion methods. Due to the presence of local minima, gradient-based methodologies are inevitably prone to errors: the system is attracted by the closest local minimum so that the final model will depend on the initial one.

In Fig. 2, a number of different V_S profiles are presented together with their Rayleigh-wave fundamental-mode dispersion curves (such a relevant V_S range is particularly emphasised by the deliberate choice of allowing a very wide range of Poisson values, thus V_P). Few straightforward observations can be depicted:

1. uncertainty increases dramatically with depth (please notice that the $\lambda/3$ - $\lambda/2$ value related to the lowest frequency - steady state approximation - provides a value of 30-45 m);
2. V_S down to about 7 m are extremely well defined;
3. due to a "compensation effect" $V_S{}^{30}$ values span in a reasonably-narrow range (272÷330 m/s, ±10% uncertainty);

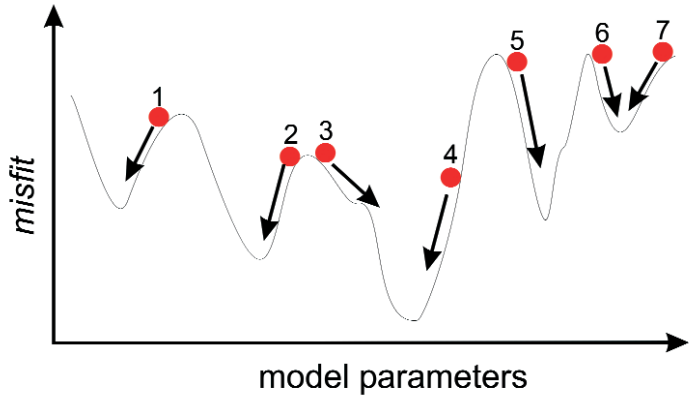

Fig. 1 - Data inversion: schematic representation of the problem caused by local minima. While using gradient-based inversion algorithms, different starting models (the numbered red circles) will provide different solutions.

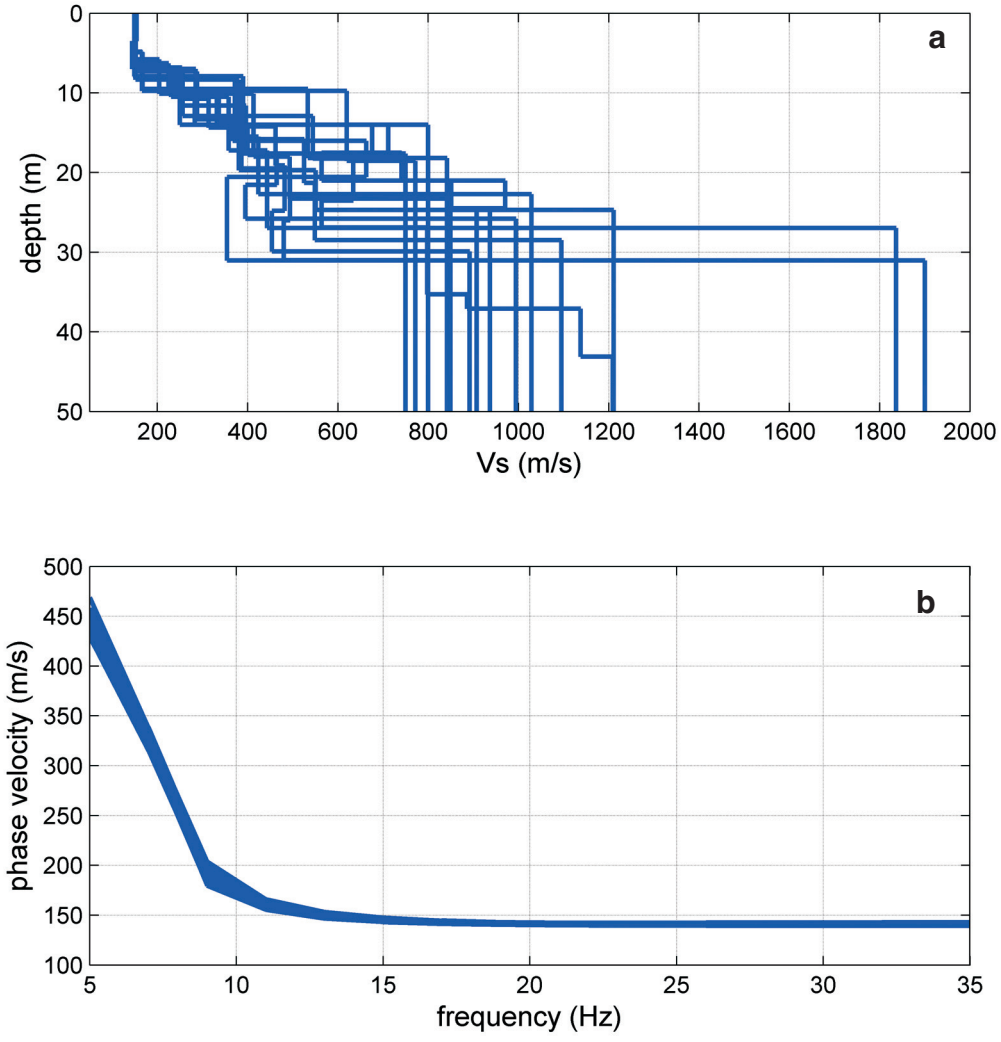

Fig. 2 - A series (a) of V_S profiles (Poisson ratios are set free to vary remarkably), and: their Rayleigh-wave fundamental-mode dispersion curves (b).

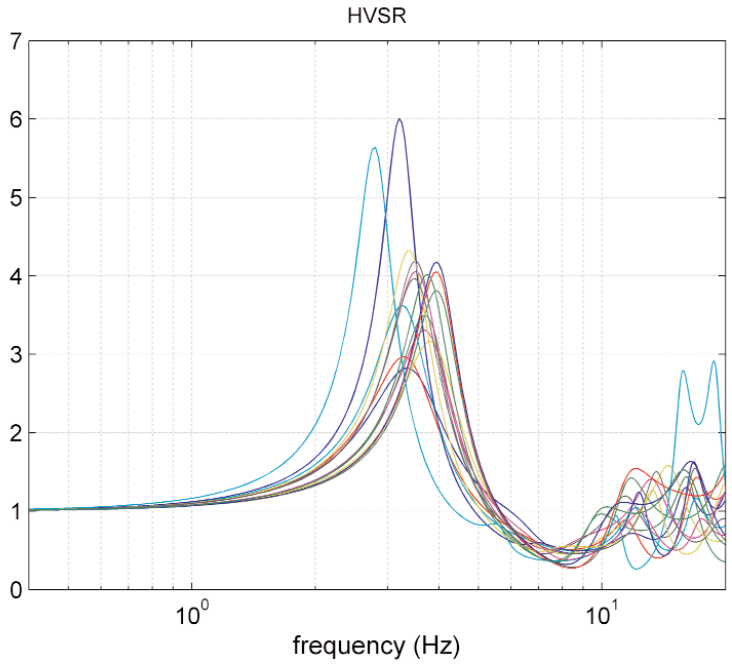

Fig. 3 - H/V curves computed (Herak, 2008) for the V_S models reported in Fig. 2.

4. the similarity of the dispersion curves of the fundamental mode is such that the models might be considered as equivalent in terms of dispersion curves (as a matter of fact extreme Poisson values can determine peculiar energy distribution among the modes, thus somehow possibly reducing this problem - see next paragraph).

It is also noteworthy that the H/V curves computed for all these models (Fig. 3), although slightly different, do not show dramatic deviations from an average characteristic peak value around 3-4 Hz.

In the last few years, several authors proposed to invert surface wave dispersion curves by means of global-search methods (e.g., Yamanaka, 2005). Although, in principle, such methods can surely better handle dispersion curve inversion, it would be quite naïf to imagine that they could represent a solution as the equivalence of the models in terms of dispersive properties (which can be thought as an extreme case of local minima) means that the right model simply does not exist.

Horizontal-to-Vertical Spectral Ratio (HVSR) - traditionally used for the estimation of the site resonance frequency - is nowadays sometimes proposed so as to depict the vertical V_S profile.

However, although HVSR jointly with dispersion curves is a remarkable tool able to better constrain possible deep horizons typically poorly-defined through dispersion curve analyses, its stand-alone application is prevented from functioning by remarkable problems related to severe non-uniqueness of the solution (Arai and Tokimatsu, 2005; Parolai *et al.*, 2005; Dal Moro, 2010).

Fig. 4 presents two models that produce identical H/V spectral ratios (many other models with similar H/V curves are clearly possible) independently from the approach used to model the H/V spectral ratios. The modelling performed by considering body waves only (Herak, 2008) shows

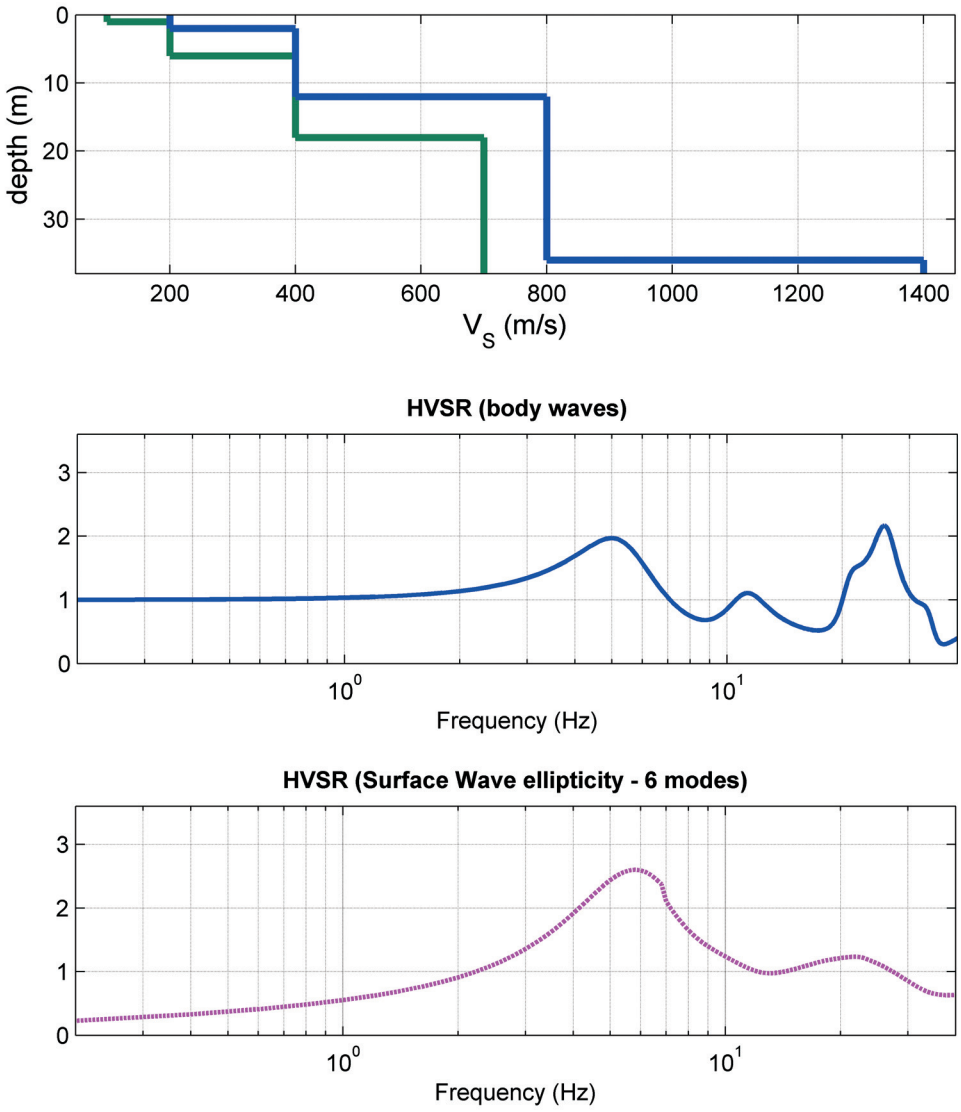

Fig. 4 – The equivalence issue in HVSR. Two V_S models (upper panels) with identical horizontal-to-vertical spectral ratio. Shown H/V curves are calculated considering body waves only (middle panel) (Herak, 2008) and SW ellipticity only (lower panel) (Lunedei and Albarello, 2009), being Q_S 10, 20, 30, 90 (Q_P=2Q_S). See text for comments.

high peaks at higher frequencies which are not present in the H/V computed considered SW ellipticity only (Lunedei and Albarello, 2009). The amplitude of the lowest peak (the fundamental period) is just slightly different for the two modelling criteria (for a review about this topic see Albarello and Lunedei, 2010).

It is then obvious that without the possibility of robustly fixing shear-wave velocities for at least the shallow layers, H/V curves are extremely ambiguous if employed for vertical V_S profiling.

A further problem is determined by the difficulties in fixing the criteria for the HVSR

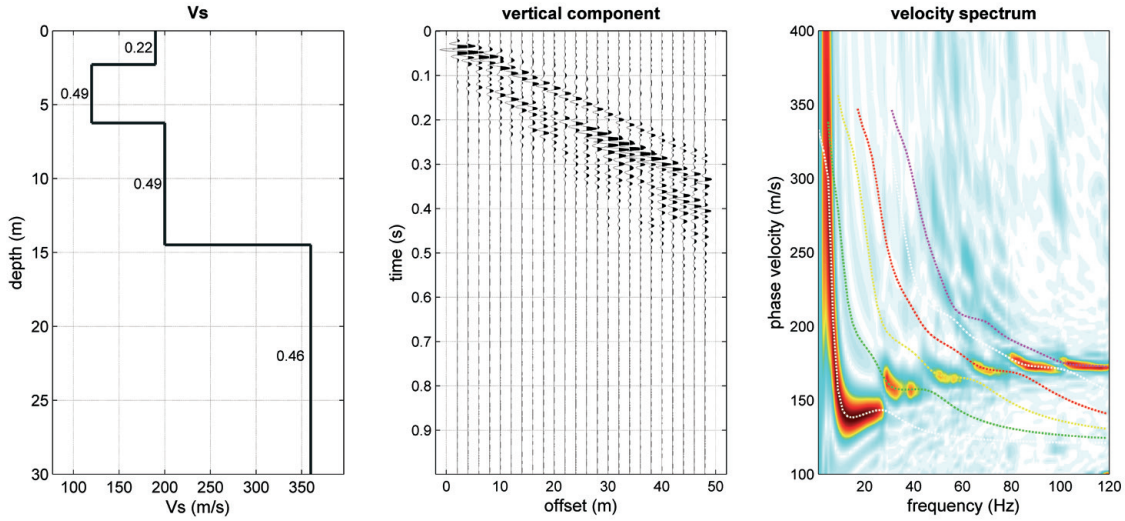

Fig. 5 - Synthetic data set (see text for details) showing an example of mode splitting: a) V_S model (reported numbers indicate the adopted Poisson values); b) seismic traces for the vertical component (vertical impact source); c) computed velocity spectrum overlapped by the theoretical Rayleigh-wave dispersion curves for the first 6 modes.

modelling which can result quite difficult when no (or little) auxiliary data are available. In fact, it becomes impossible to determine *a priori* the relative importance of Rayleigh, Love and body waves (e.g., Fah *et al.,* 2001; Bonnefoy-Claudet *et al.*, 2006, 2008), the number of relevant surface wave modes and the influence of the quality factors Q (Lunedei and Albarello, 2009). Please notice that these aspects appear to be typically site dependant, so no universal solution can be considered valid (see also the case study presented later on).

Some problems related to the stability of the H/V spectral ratio also arise. It is for instance well known that, especially at the lowest frequencies, weather conditions may affect the microtremor spectra (e.g., Tanimoto, 1999; Ali *et al.*, 2010) and that artificial sources (such as industrial facilities, etc.) introduce signals that, if not properly filtered out, risk to be interpreted in terms of subsurface structure.

Joint inversion of different kinds of seismic data is thus a remarkable way both to reduce non-uniqueness of the solution and give a sounder data interpretation (e.g., Picozzi and Albarello 2007; Dal Moro, 2008, 2010).

Because of the problems caused by the presence of local minima and the equivalence of the solutions (please notice that, although clearly related, these problems are different) it is the responsibility of the interpreter to choose a model which holds a geological and stratigraphical meaning [“We do not invert. We model”: Stokoe (2009)].

3. Modal energy distribution in surface wave propagation

While analyzing field data sets, a proper and sound data interpretation (i.e., mode

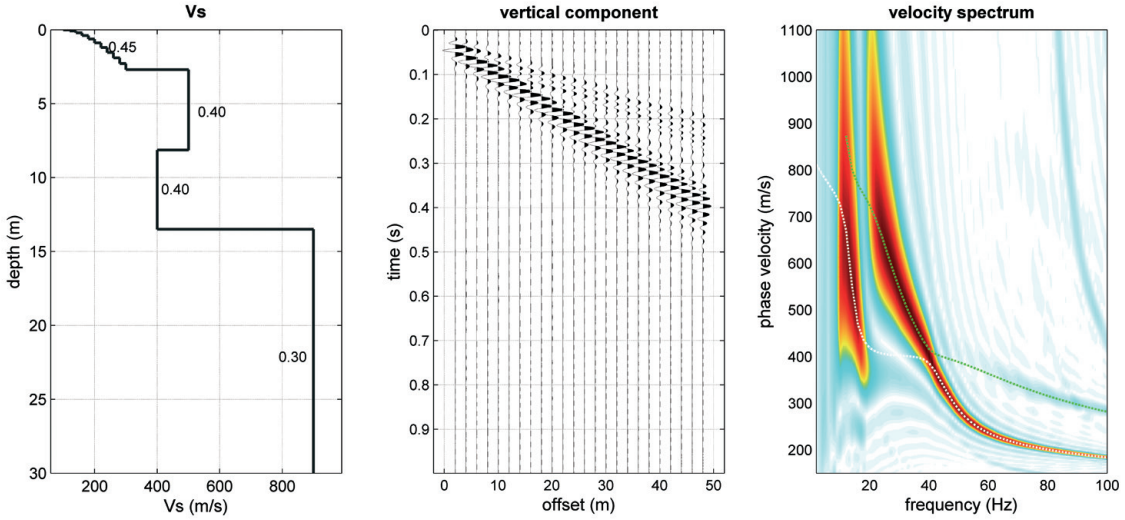

Fig. 6 - Synthetic data set: a) V_S model (reported numbers indicate the adopted Poisson values); b) seismic traces for the vertical component (vertical impact source); c) computed velocity spectrum overlapped by the theoretical Rayleigh-wave dispersion curves for the first 2 modes.

identification) is clearly necessary but when energy distribution among different modes does not follow elementary patterns, data interpretation might become problematic.

In order to show how different modes can actually roll up, a series of synthetic seismograms

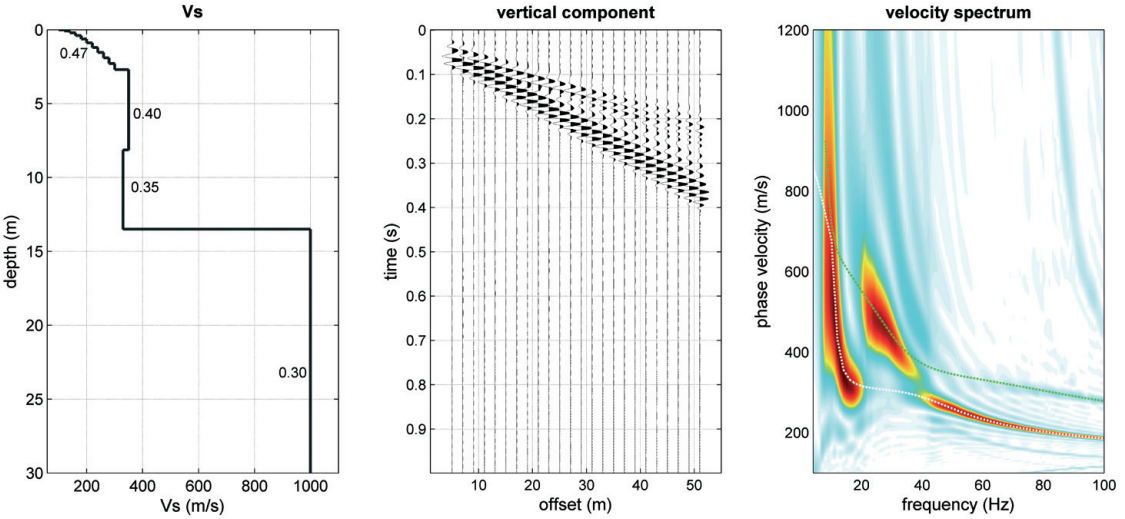

Fig. 7 - Synthetic data set: a) V_S model (reported numbers indicate the adopted Poisson values); b) seismic traces for the vertical component (vertical impact source); c) computed velocity spectrum overlapped by the theoretical Rayleigh-wave dispersion curves for the first 2 modes.

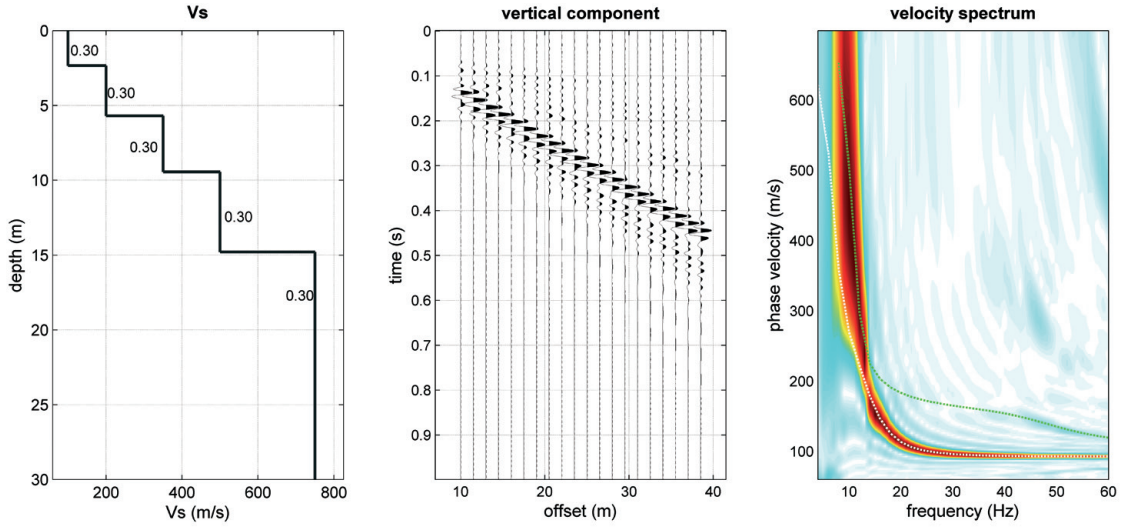

Fig. 8 - Synthetic data set: a) V_S model (reported numbers indicate the adopted Poisson values); b) seismic traces for the vertical component (vertical impact source); c) computed velocity spectrum overlapped by the theoretical Rayleigh-wave dispersion curves for the first 2 modes.

were computed by means of the computational scheme proposed by Carcione (1992).

Four data sets are presented. For each of them V_S profiles (and adopted Poisson moduli) are reported together with computed seismic traces (Figs. 5, 6, 7 and 8). Theoretical Rayleigh-wave dispersion curves computed according to Dunkin (1965) are overlapped with the computed velocity spectra.

The model reported in Fig. 5 shows an example of so-called “mode splitting”. Fundamental mode dominates up to about 28 Hz while for higher frequencies the energy pertains to higher and higher modes within small and clearly defined frequency ranges.

Data reported in Fig. 6 put in evidence the fact that fundamental and higher modes can merge and appear as a single mode. The fundamental mode disappears at about 20 Hz and re-appears for frequencies higher than 40 Hz. At this point, a first higher mode merges with the fundamental one determining a signal that might be (mis)interpreted as if related to a single mode.

Fig. 7 shows an example of a double mode jump since the fundamental mode dominates for frequencies higher than 40 and lower than 20 Hz, while the energy in between is due to the first higher mode. Synthetic data reported in Fig. 8 show that, under some circumstances which cannot be universally simplified, mode jumps are possible even when no velocity inversion occurs (please notice that the energy that dominates for frequencies lower than about 14 Hz relates to the first higher mode).

The first field data set considered (Fig. 9) was acquired in an alluvial plain in north-eastern Italy. The energy distribution is in principle quite similar to the one calculated for the synthetic data set reported in Fig. 7 where energy is distributed among different modes.

Another field data set, acquired close to Pisa (Italy) and presented in Fig. 10, shows a remarkable phenomenon of mode splitting (compare with the synthetic data in Fig. 5).

Mode jumping is then a phenomenon that can occur more than once in the same data set and

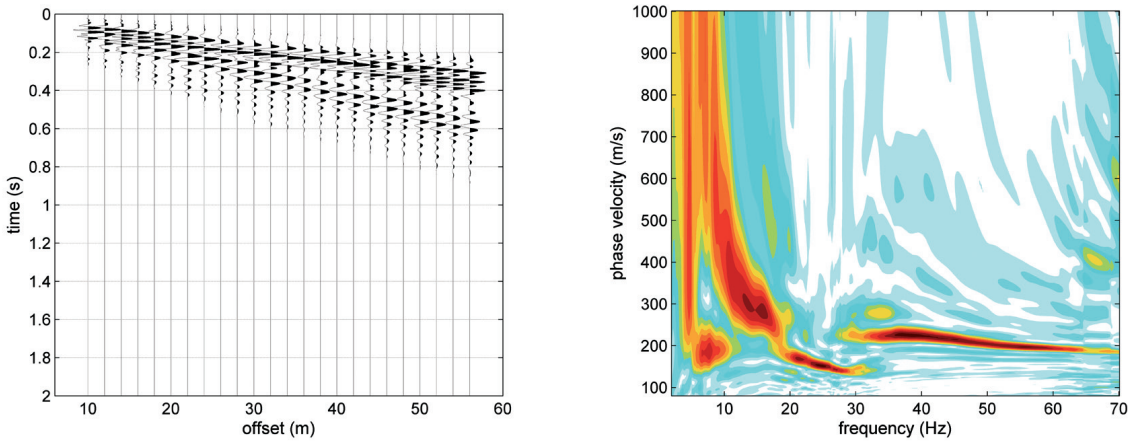

Fig. 9 – MASW field data set: acquired traces (vertical component, vertical-impact sledgehammer) and computed velocity spectrum. Notice the energy associates with higher modes in the 10-20 Hz range and for frequencies higher than 30 Hz.

energy can distribute itself over different modes in a complex, yet interpretable, fashion.

It must be underlined that once properly interpreted, higher modes do not represent a class of noise but valuable information that is extremely important to better define the subsurface model, in particular for the deeper layers (Xia *et al.*, 2003).

Crucial elements typically (but not necessarily nor uniquely) responsible for complex energy distribution (i.e., mode jumps) are velocity inversions and high Poisson values - see reported synthetic data sets and compare with O'Neill *et al.* (2004) and O'Neill and Matsuoka (2005).

The synthetic and field data presented here show that the velocity spectra must be carefully

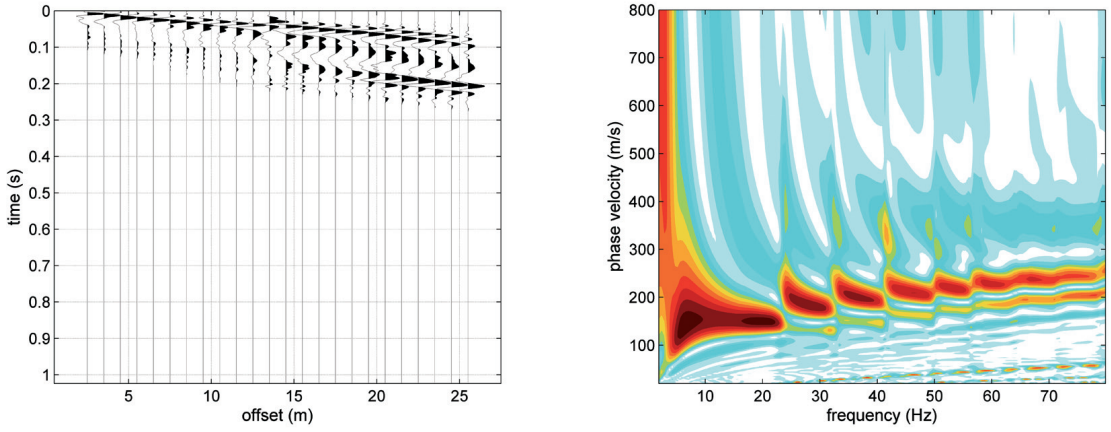

Fig. 10 – MASW field data set: remarkable example of mode splitting (courtesy of Studio di Geologia Stefania Botti, Sarzana - La Spezia, Italy).

Table 1 - Acquisition parameters for the MASW and ReMi field data sets.

	MASW (Rayleigh & Love)	ReMi (Rayleigh)
Minimum offset	4 m	-
Receiver spacing (24 channels)	2 m	2 m
Sample interval	0.125 ms	0.25 ms
Acquisition length	2 s	600 s

evaluated to be properly interpreted. In fact, too often, implicitly proposed paradigms about energy distribution state that the fundamental mode is the most energetic one and that higher modes usually appear only at higher frequencies. The results presented show that these assumptions do not necessarily apply and may mislead velocity spectra interpretations.

Although joint inversion of fundamental and higher modes is easily performed in the framework of different possible inversion schemes (e.g., Xia *et al.*, 2003; Dal Moro *et al.*, 2007) the critical point that we wish to underline is about their proper interpretation as possible misinterpretations necessarily lead to inaccurate V_S profiles (e.g., Zhang and Chan, 2003). Velocity spectra interpretation is often a non-trivial task that should be performed with care, being aware that the results of any inversion process are first of all determined by that rather than by the robustness of the adopted inversion algorithm.

4. Joint analysis: a case study

Due to the problems described in the previous sections, a series of field data sets were acquired with the aim of retrieving a subsurface model coherent with all the observed data, thus reducing the otherwise inevitable ambiguities. The chosen site is located in north-eastern Italy in a upper plain area where the stratigraphical sequence is basically composed of silty and sandy layers with occasional variously-cemented gravel lens. In particular, a superficial and abrupt V_S contrast determined by the contact between silty layers and gravels produces some peculiarities that make the site particularly interesting.

Acquisition parameters for the MASW and ReMi data sets are reported in Table 1. Rayleigh and Love waves were acquired using 4.5 Hz vertical and horizontal geophones respectively. A sledgehammer was used as a source: vertical impact for Rayleigh waves, horizontal (shear source) for Love waves. HVSR was computed according to the SESAME guidelines (SESAME, 2005) by considering a 20 minute microtremor data set with a sample rate of 2 ms (acquisition was performed by means of a calibrated three-component geophone).

Acquired multi-channel data were processed in order to evaluate Rayleigh and Love-wave dispersion properties, V_P and V_{SH} refraction travel times and Rayleigh-wave attenuation.

Compressional and shear (SH) wave refraction analyses on first arrivals (Fig. 11) were used to characterize the shallowest layers and furnish V_S and V_P values to compare and use while analysing SW dispersion and HVSR. In fact, velocity spectra (especially for Rayleigh waves) show complex mode interplay (see Fig. 13, left column) and HVSR, to be properly interpreted,

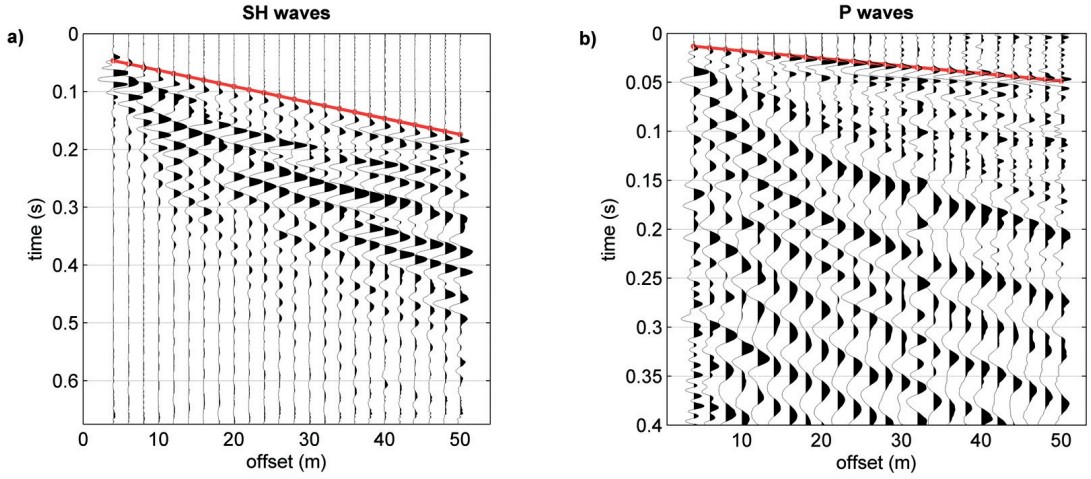

Fig. 11 - Refraction data. Left and right panels report the transversal (SH) and vertical (P) data sets respectively. First arrivals show a clear horizon at about 4 m depth (V_S: 120, 190, 380 m/s; V_P: 300, 480, 1800 m/s; thickness: 1, 3 m).

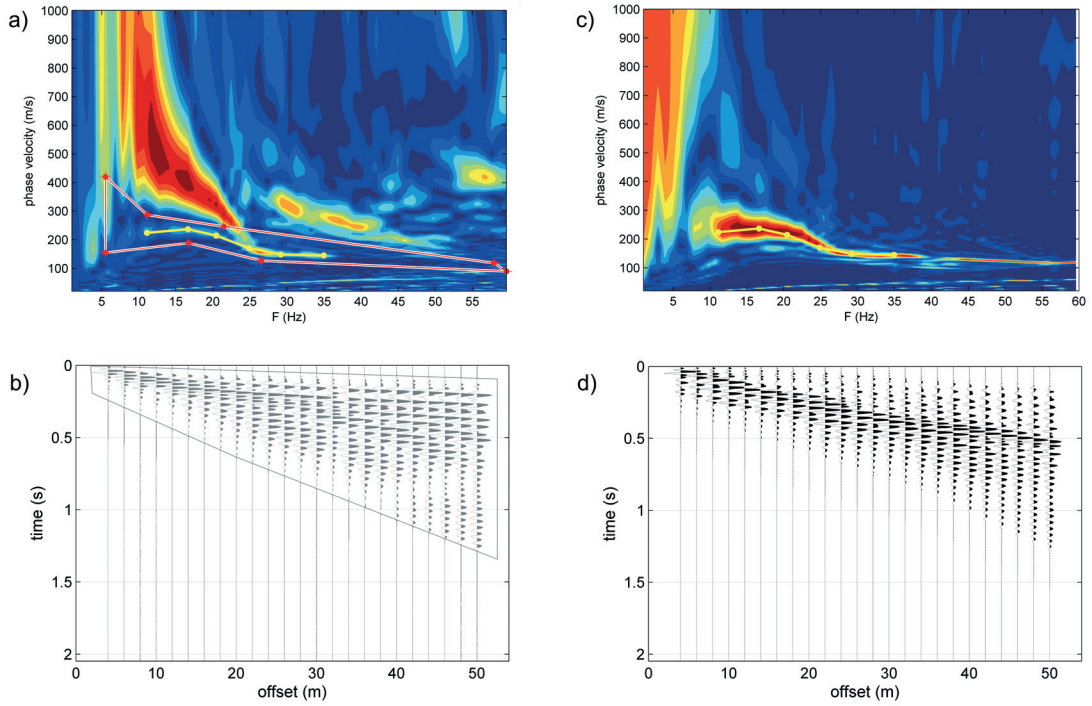

Fig. 12 - Rayleigh-wave fundamental-mode separation: a) raw-data velocity spectrum with overlapped by the polygon used to filter out the signals not related to the fundamental mode; b) raw data in the *x-t* domain (the polygon shows Rayleigh-wave propagation); c) velocity spectrum of the filtered data; d) filtered data in the *x-t* domain. The yellow curve is the dispersion curve pertinent to the fundamental mode (quite weak in the raw data).

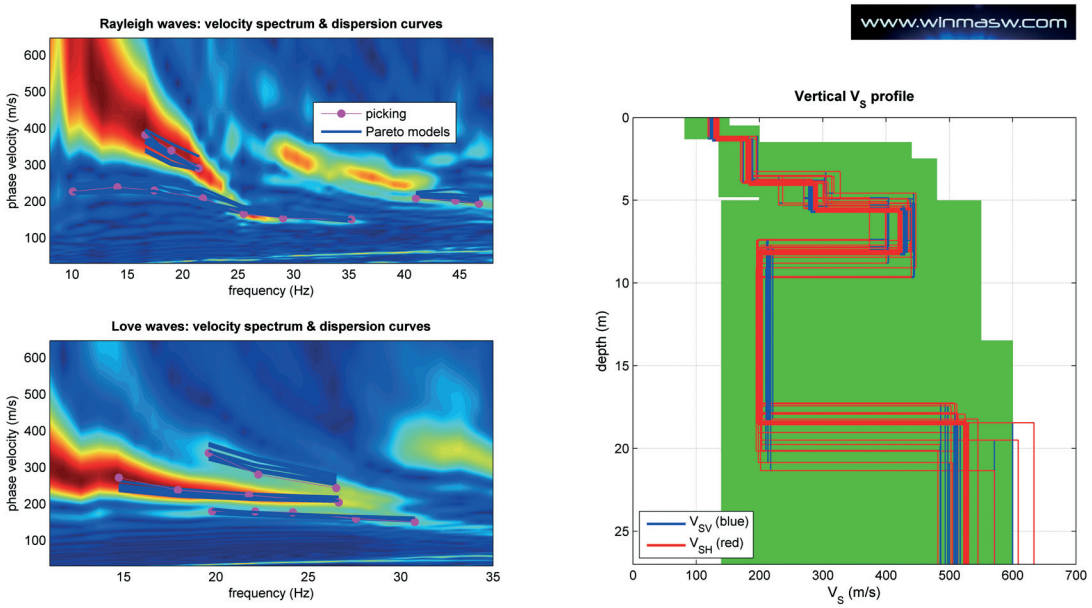

Fig. 13 – Joint analysis of Rayleigh and Love dispersion curves. On the left: top and bottom panels present the velocity spectra together with the picked and inverted (Pareto front models) dispersion curves for Rayleigh and Love waves respectively. On the right: V_S profiles for the Pareto front models.

required sound and quantitative constraints at least for the superficial layers.

V_{SH} values identified through SH-wave refraction analyses are useful to confirm the interpretation of the velocity spectrum during MASW analyses. In fact, thanks to these values, we can corroborate the interpretation that the energy which is particularly evident between 25 and 35 Hz (see Fig. 12a) in the vertical-component spectrum (related to Rayleigh waves) is attributable to the fundamental mode. The fundamental mode is actually present as a faint signal also in the 8-25 Hz range, showing phase velocities of about 150-230 m/s with clear evidence of inverse dispersion (see also Fig. 13, left column).

In the horizontal (transversal) component (related to Love waves) the fundamental mode appears particularly evident in the 20-33 Hz frequency range (Fig. 13 left column).

The complex energy distribution among different modes is mostly due to the superficial high V_S contrast already put in evidence by the refraction travel time analysis.

The energy that dominates the vertical-component spectrum (Rayleigh waves) in the 9-24 Hz frequency range is due to higher modes and cannot be attributed to guided waves as these have peculiar characteristics that are quite different from the observed ones (Robertsson *et al.*, 1996; Roth and Holliger, 1999).

Analogously to the velocity spectrum derived from the MASW acquisition (Rayleigh component), the velocity spectrum determined via ReMi acquisitions (Fig. 15) still appears dominated by higher modes.

Before picking the dispersion curves pertinent to the different modes present in the data sets, data were filtered in the *f-k* domain (Yilmaz, 1987) in order to separate (thus putting in evidence)

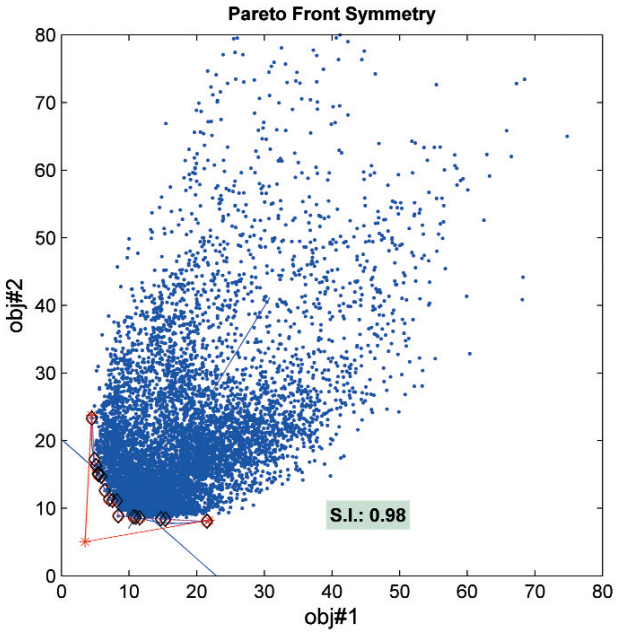

Fig. 14 – Joint inversion of Rayleigh- and Love-wave dispersion curves. Distribution of the evaluated models in the bi-objective space (obj#1: Rayleigh-wave misfit; obj#2: Love-wave misfit). Symmetry Index (S.I.) of the Pareto front models (red circles) is also reported (see text for details).

signals related to weak modes (see also Luo *et al.*, 2009). In particular, Fig. 12 reports the Rayleigh-wave data set both in the *x-t* and *v-f* domains before and after the performed processing. The fundamental mode that was quite evanescent in the original data set now results clearly quite apparent. Similar processing was considered while analysing dispersive properties of Love waves.

Joint multimodal inversion performed via a Multi-Objective algorithm based on the Pareto front evaluation (Dal Moro and Pipan, 2007; Dal Moro, 2008, 2010; Dal Moro and Ferigo, 2011). The results (Figs. 13 and 14) show an overall consistency also confirmed by the very high Symmetry Index (theoretically ranging between –1 and 1) (variability of the V_S profiles of the Pareto front models reported in Fig. 13 shows the uncertainty of the retrieved model). This is given by the scalar product between the axis of the full set of evaluated models and the symmetry axis of the Pareto front [for details see Dal Moro and Ferigo (2011)]. In fact, the symmetry of the Pareto front models with respect to the universe of considered models is an index of the general consistency of the whole inversion process (thus of the data interpretation and final results as well).

A further validation of the overall congruency of the shallowest part of the model is furnished by the analysis of the Rayleigh-wave attenuation (e.g., Xia *et al.*, 2002). Fig. 16 reports the Q_S model together with the observed and calculated attenuation curves as a function of frequency and $\lambda/2$. The presence of a highly attenuating 4-m thick material lying over a high-Q_S layer is apparent and further supports the proposed model. While quality factors down to about 8 m are well determined, values related to deeper layers must be considered as highly speculative due to the limitations of the method.

Fig. 17 reports the V_S model (the values down to about 22 m refer to the joint SW inversion presented in Fig. 13) and the observed and calculated HVSR computed while adopting different

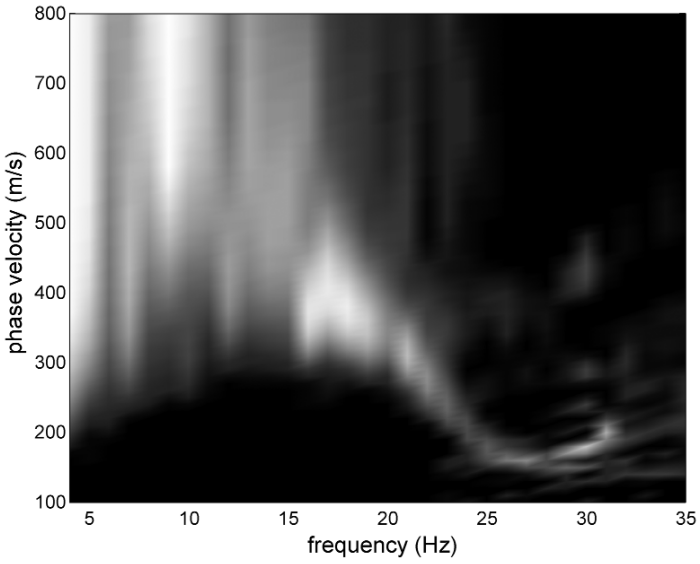

Fig. 15 - Velocity spectrum determined through ReMi acquisitions. Notice that, similarly to MASW data (Rayleigh component), higher modes

possible criteria. Please notice that the observed pick at about 1 Hz (signal A) is due to an industrial facility a few hundred meters from the investigated site and not to a lithological horizon.

Together with the observed curve, Fig. 17b reports synthetic HVSR computed while considering body waves (Herak, 2008) and SW ellipticity (Lunedei and Albarello, 2009) in the framework of the elastic case. HVSR is computed by considering only the first 2 modes (both Rayleigh and Love waves are considered). Fig. 17c reports the same data while considering the quality factors reported in Figs. 16 and 10 modes for the HVSR modelling computed via SW ellipticity.

It is apparent that for the present site the second case is more appropriate. While the

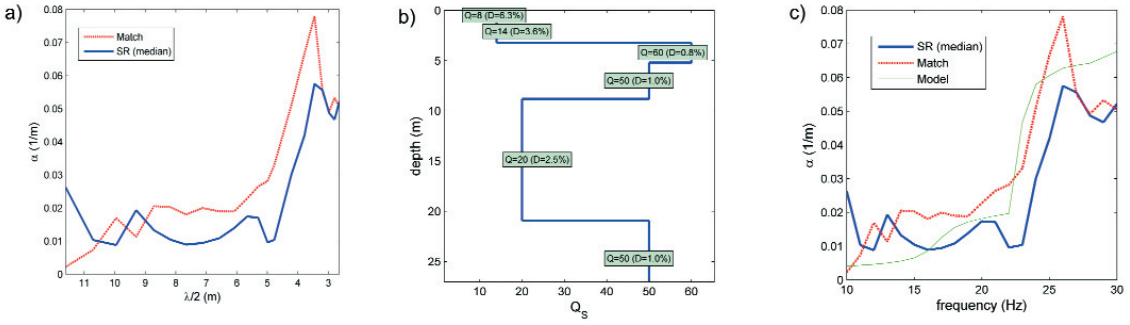

Fig. 16 - Rayleigh-wave attenuation analyses: a) attenuation curve as a function of $\lambda/2$; b) Q_S model; c) observed curves calculated according to spectral ratio and matching technique (Tonn, 1991) together with the attenuation curve of the proposed model.

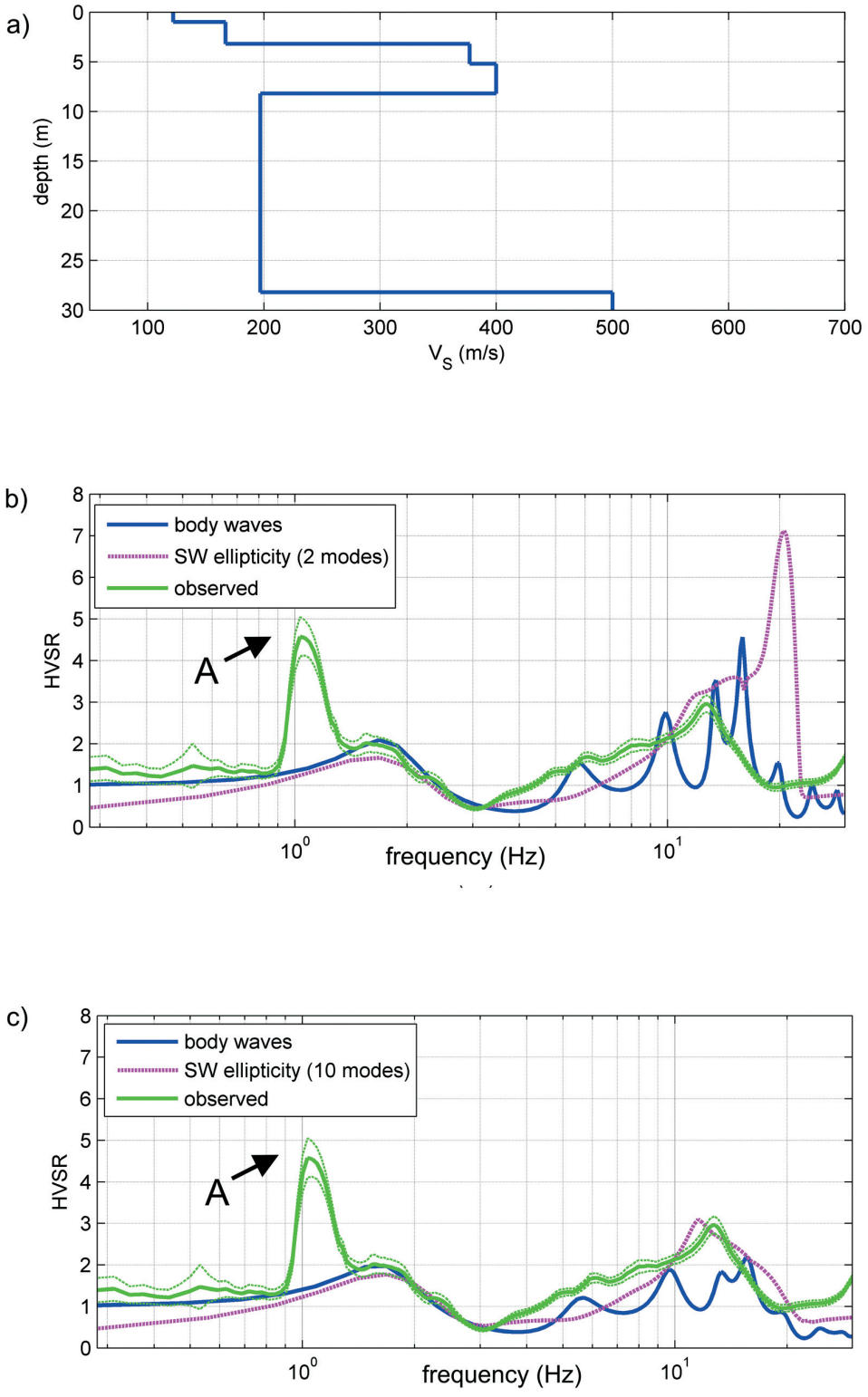

Fig. 17 - HVSR. Green: observed data; magenta: theoretical H/V curves while considering SW ellipticity; blue: theoretical H/V while considering body waves. See text for details.

fundamental period (the peak centred at 1.6 Hz and related to the 28-m deep horizon) is equally reproduced both by body waves and SW ellipticity, for frequencies higher than 3 Hz most of the H/V curve is better approximated by the SW ellipticity computed adopting a high number of modes also considering the attenuation (compare Figs. 17b and 17c).

5. Conclusions

After having summarized some problems related to surface non-invasive methods for near-surface investigations, a case study was presented with the aim of showing some complexities that if improperly interpreted would lead to erroneous subsurface reconstruction.

The overall goal was to put in evidence the fact that assumptions (often implicitly) considered while performing near-surface seismic data interpretation and modelling should be carefully checked before delivering a model and the only way to do that is by carrying out a joint analysis.

Velocity spectra obtained by means of MASW analyses can show complex mode interlacing while velocity spectra determined via ReMi acquisitions are necessarily blurred and fuzzy. In any case, the assumption often adopted that the fundamental mode dominates the data can be erroneous in both cases.

In the last decade, we witnessed a flourishing of papers on global search methods for dispersion curve inversion. Due to severe non-uniqueness of the solution (different models can be equivalent in terms of SW dispersion), they cannot be claimed as the solution even if, especially in case of strong impedance contrasts, their heavier computational effort can provide more accurate solutions. A question such as "is the inversion scheme able to retrieve the right model?" results quite dull because, as shown in the second paragraph, especially in case of inversion schemes based on the fundamental mode only the equivalence of different models makes such a point meaningless.

Even though extremely useful for imaging deeper layers, HVSR cannot provide unambiguous V_S values when not supported by detailed superficial V_S values given by SW dispersion and/or SH-wave refraction/reflection studies. Moreover, some aspects related to the HVSR modelling [role of Love waves, higher modes, quality factors and body waves: e.g., Bonnefoy-Claudet *et al.* (2008), Albarello and Lunedei (2010), Dal Moro (2010)] pose some problems that can be addressed only by adopting a holistic approach (see e.g., the presented case study).

Consequently, especially in case of complex data sets that can turn out to be quite challenging in terms of velocity spectra interpretation and HVSR modelling criteria, if we are interested in an unambiguous site characterization (e.g., for geotechnical purposes) the only way to approach the problem is to preform a joint analysis of all suitable data. In fact, if a non-holistic approach is adopted, there would be no chance of cross-validating data interpretation, model parameters and modelling criteria.

A joint analysis of Rayleigh and Love-wave dispersion curves (possibly together with SH-wave reflection/refraction analyses) can moreover provide quantitative information about possible anisotropies which would reflect in different shear-wave velocities, being that Rayleigh-wave dispersion depends on V_{SV} while Love-wave dispersion and SH-wave reflection/refraction on V_{SH} (e.g., Gaherty, 2004; Safani *et al.*, 2005).

The case study considered also supports the idea that although at high frequencies, SW

ellipticity is the driving force which determines the observed HVSR (see Fig. 17 at frequencies higher than 3 Hz), the H/V curve for the fundamental period may be (sometimes better) approximated by body-wave based modelling (peak at 1.6 Hz in Fig. 17) - see also Albarello and Lunedei (2010) and Dal Moro (2010).

Acknowledgements. The present work was partially presented during the annual GNGTS Congress (November 16-19, 2009, Trieste, Italy). Part of the work was conducted in the framework of the following research grants: COFIN 2006 (prof. Pipan); ASSESS project - Protezione Civile del Friuli Venezia Giulia. Data presented in Fig. 10 were kindly provided by Studio di Geologia Stefania Botti (Sarzana - La Spezia, Italy). Special thanks to Fulvio Podda for his friendship and help during the acquisition campaign.

REFERENCES

Albarello D. and Lunedei E.; 2010: *Alternative interpretations of horizontal to vertical spectral ratios of ambient vibrations: new insights from theoretical modeling.* Bull. Earthquake Eng., **8**, 519–534.

Ali M.Y., Berteussen K., Small J. and Barkat B.; 2010: *Low-frequency passive seismic experiments in Abu Dhabi, United Arab Emirates: implications for hydrocarbon detection.* Geophys. Prosp., **58**, 875-899.

Arai H. and Tokimatsu K.; 2005: *S-Wave velocity profiling by joint inversion of microtremor dispersion curve and horizontal-to-vertical (H/V) spectrum.* Bull. Seism. Soc. Am., **95**, 1766-1778.

Bonnefoy-Claudet S., Cotton F. and Bard P.Y.; 2006: *The nature of noise wavefield and its applications for site effects studies: a literature review.* Earth-Science Reviews, **79**, 205-227.

Bonnefoy-Claudet S., Köhler A., Cornou C., Wathelet M. and Bard P.Y.; 2008: *Effects of Love waves on microtremor* H/V *ratio.* Bull. Seism. Soc. Am., **98**, 288-300.

Carcione J.M.; 1992: *Modeling anelastic singular surface waves in the Earth.* Geophysics, **57**, 781-792.

Dal Moro G.; 2008: *V_S and V_P vertical profiling and poisson ratio estimation via joint inversion of Rayleigh waves and refraction travel times by means of bi-objective evolutionary algorithm.* Jour. Appl. Geophys., **66**, 15-24.

Dal Moro G.; 2010: *Insights on surface-wave dispersion curves and* HVSR*: joint analysis via Pareto optimality.* Jour. Appl. Geophys., **72**, 29-140.

Dal Moro G. and Ferigo F.; 2011: *Joint analysis of Rayleigh and Love-wave dispersion curves: issues, criteria and improvements.* In preparation.

Dal Moro G. and Pipan M.; 2007: *Joint inversion of surface wave dispersion curves and reflection travel times via multi-objective evolutionary algorithms.* Jour. Applied Geophysics, **61**, 56-81.

Dal Moro G., Pipan M. and Gabrielli P.; 2007: *Rayleigh wave dispersion curve inversion via genetic algorithms and marginal posterior probability density estimation.* J. App. Geophys., **61**, 39-55.

Dunkin J.W.; 1965: *Computation of modal solutions in layered, elastic media at high frequencies.* Bull. Seism. Soc. Am., **55**, 335-358.

Fah D., Kind F. and Giardini D.; 2001: *A theoretical investigation of average* H/V *ratios.* Geophys. Jour. Int., **145**, 535-549.

Gaherty J.B.; 2004: *A surface wave analysis of seismic anisotropy beneath eastern North America.* Geophys. Jour. Int., **158**, 1053-1066.

Glangeaud F., Mari J., Lacoume J.L., Mars J. and Nardin M.; 1999: *Dispersive seismic waves in geophysics.* European Jour. of Environmental and Engineering Geophys., **3**, 265-306.

Herak M.; 2008: *Model* HVSR *- A Matlab tool to model horizontal-to-vertical spectral ratio of ambient noise*.

Computers and Geosciences, **34**, 1514-1526.

Ivanov J., Miller R.D., Xia J., Steeples D.W. and Park C.B.; 2005a: *The inverse problem of refraction traveltimes, part I: types of geophysical non uniqueness through minimization.* Pure and Appl. Geophys., **162**, 447-459.

Ivanov J., Miller R.D., Xia J. and Steeples D.; 2005b: *The inverse problem of refraction traveltimes, part II: Quantifying refraction non uniqueness using a three-layer model*. Pure Appl. Geophys., **162**, 461-477.

Louie J.N.; 2001: *Faster, better: shear-wave velocity to 100 meters depth from refraction microtremor arrays.* Bull. Seism. Soc. Am., **91**, 347-364.

Luke B., Calderón-Macías C., Stone R. C. and Huynh M.; 2003: *Nonuniqueness in inversion of seismic surface-wave data*. In: Proceedings of the symposium on the application of geophysics to engineering and environmental problems: Environmental and Engineering Geophysical Society, CD-ROM SUR05.

Lunedei E. and Albarello D.; 2009: *On the seismic noise wavefield in a weakly dissipative layered Earth.* Geophys. Jour. Int., **177**, 1001-1014.

Luo Y., Xia J., Miller R.D., Xu Y., Liu J. and Liu Q.; 2009: *Rayleigh-wave mode separation by high-resolution linear Radon transform.* Geophys. J. Int., **179**, 254-264.

O'Neill A. and Matsuoka T.; 2005: *Dominant higher surface-wave modes and possible inversion pitfalls*. Jour. of Environmental and Engineering Geophys., **10**, 185-201.

O'Neill A., Matsuoka T. and Tsukada K.; 2004: *Some pitfalls associated with dominant higher-mode surface-wave inversion.* In: Near Surface 2004, 10th meeting of the European Association of Geoscientists and Engineers (EAGE), 6-9 September 2004, Utrecht, The Netherlands, Z-99.

O'Neill A., Safani J., Matsuoka T. and Shiraishi K.; 2006: *Rapid shear wave velocity imaging with seismic landstreamers and surface wave inversion.* Exploration Geophys., **37**, 292-306.

Park C.B., Miller R.D. and Xia J.; 1999: *Multichannel analysis of surface waves.* Geophysics, **64**, 800-808.

Parolai S., Picozzi M., Richwalski S.M. and Milkereit C.; 2005: *Joint inversion of phase velocity dispersion and H/V ratio curves from seismic noise recordings using a genetic algorithm, considering higher modes.* Geophs. Res, Lett., **32**, L01303.

Picozzi M. and Albarello D.; 2007: *Combining genetic and linearized algorithms for a two-step joint inversion of Rayleigh wave dispersion and* H/V *spectral ratio curves.* Geophys. Jour. Int., **169**, 189-200.

Robertsson J.O.A., Holliger K. and Green A.G.; 1996: *Source-generated noise in shallow seismic data.* European Jour. of Environamental and Engineering Geophys., **1**, 107-124.

Roth M. and Holliger K.; 1999: *Inversion of source-generated noise in high-resolution seismic data.* The Leading Edge, **18**, 1402-1406.

Safani J., O'Neill A., Matsuoka T. and Sanada Y.; 2005: *Applications of Love wave dispersion for improved shear-wave velocity imaging.* Jour. of Environmental and Engineering Geophys., **10**, 135–150.

Scales J.A., Smith M.L. and Treitel S.; 2001: *Introductory geophysical inverse theory*. Samizdat Press, 193 pp., <http://samizdat.mines.edu>.

SESAME; 2005: *Guidelines for the implementation of the H/V spectral ratio technique on ambient vibrations measurements.* In: Processing and Interpretation, <http://sesame-fp5.obs.ujf-grenoble.fr/Papers/HV_User_Guidelines.pdf >.

Shtivelman V.; 1999: *Using surface waves for estimating the shear-wave velocities in the shallow subsurface onshore and offshore Israel.* Eur. J. Environ. Eng. Geophys., **4**, 17-36.

Shtivelman V.; 2002: *Surface wave sections as a tool for imaging subsurface inhomogeneities.* Europ. Jour. of Environmental and Engineering Geophys., **7**, 121–138.

Stokoe K.H.; 2009: *Sesimic and laboratory seismic measurements in civil engineering applications.* In: O'Connor P. (ed), Near Surface 2009, 15th meeting of the European Association of Geoscientists and Engineers (EAGE), 7-9 September 2009, Dublin, Ireland.

Stokoe K.H. II, Nazarian S., Rix G.J., Sanchez-Salinero I., Sheu J. and Mok Y.; 1988: *In situ seismic testing of hard-to-sample soils by surface wave method.* In: Proceeding, Earthquake Eng. and Soil Din. II: Recent Advances in Ground Motion Evalutation, Special Pubbl. 20, ASCE, Park City, pp. 264-277.

Tanimoto T.; 1999: *Excitation of normal modes by atmospheric turbulence: source of long-period seismic noise.* Geophys. Jour. Int., **136**, 395–402.

Tonn R.; 1991: *The determination of the seismic quality factor Q from VSP data: a comparison of different*

computational methods. Geophysical Prospecting, **39**, 1-27.

Xia J., Miller R.D. and Park C.B.; 1999: *Estimation of near-surface shear-wave velocity by inversion of Rayleigh waves.* Geophysics. **64**, 691-700.

Xia J., Miller R.D., Park C.B., Ivanov J., Tian G. and Chen C.; 2004: *Utilization of high-frequency Rayleigh waves in near-surface geophysics.* The Leading Edge, **23**, 753-759.

Xia J., Miller R.D., Park C.B. and Tian G.; 2002: *Determining Q of near-surface materials from Rayleigh waves.* J. Appl. Geophys., **51**, 121– 129.

Xia J., Miller R.D., Park C.B. and Tian G.; 2003: *Inversion of high frequency surface waves with fundamental and higher modes.* Jour. of Appl. Geophys., **52**, 45–57.

Yamanaka H.; 2005: *Comparison of Performance of Heuristic Search Methods for Phase Velocity Inversion in Shallow Surface Wave Method.* Jour. of Environmental and Engineering Geophys., **10**, 163–173.

Yilmaz O.; 1987: *Seismic data processing.* Society of Exploration Geophysicists, Tulsa Oklaoma, 526 pp.

Zhang S.X. and Chan L.S.; 2003: *Possible effects of misidentified mode number on Rayleigh wave inversion.* Jour. of Appl. Geophys., **53**, 17-29.

Corresponding author: Giancarlo Dal Moro
Eliosoft
Via Palmanova 18/G, 33057 Palmanova (UD), Italy
Phone: +39 328 2510528; e-mail: gdm@winmasw.com